Electronic Supplementary Information

Perovskite $KNi_{0.8}Co_{0.2}F_3$ nanocrystals for supercapacitors

Rui Ding*, Xudong Li, Wei Shi, Qilei Xu, Xiuli Han, Yong Zhou, Weifeng Hong, Enhui Liu

Key Laboratory of Environmentally Friendly Chemistry and Applications of Ministry of Education,

College of Chemistry, Xiangtan University, Hunan 411105, P.R. China

* E-mails: drm8122@163.com; drm8122@xtu.edu.cn (R. Ding);

Tel: +86 731 58292202; Fax: +86 731 58292251

Experimental

Synthesis of K-Ni-Co-F materials

All chemicals in the study were of analytical grade (A.R.). The K-Ni-Co-F materials with various Ni/Co ratios (1:0, 8:1, 4:1, 2:1, 1:1 ,1:2, 0:1) were prepared via a facile solvothermal route. Take the procedure of K-Ni-Co-F (Ni/Co=4:1) for an example. Firstly, 1.6 mmol $NiCl_2$•$6H_2O$, 0.4 mmol $CoCl_2$•$6H_2O$ and 5 mmol KF•$2H_2O$ were dissolved into 40 mL ethylene glycol (EG), which was magnetically stirred and dispersed in an ultrasonic bath for 30 min; Secondly, the mixture was transferred into a 50 mL Teflon-lined stainless steel autoclave, which was heated at 180 ^{o}C for 24 h in an oven, and then cooled down naturally; Finally, the precipitates were collected by centrifugal filtration and dried at 100 ^{o}C overnight to obtain the products. The other K-Ni-Co-F materials (Ni/Co=1:0, 8:1, 2:1, 1:1 ,1:2, 0:1) were also prepared simply by varying the Ni/Co molar ratios.

Characterizations

The phase compositions and crystallinity were checked by X-ray diffraction (XRD). The surface chemical compositions and electronic structures were measured by X-ray photoelectron spectra (XPS). The morphology and size was observed by scanning electron microscopy (SEM) and transmission electron microscopy (TEM). The crystalline microstructures were examined by the high-resolution TEM (HRTEM) and selected area electron diffraction (SAED). The element composition and distribution were determined by the energy dispersive X-ray spectra (EDS) and mapping. The specific surface area and pore size distribution were tested by nitrogen sorption measurements with Brunauer-Emmett-Teller (BET) and Barrett-Joyner-Halenda (BJH) methods.

Electrochemical measurements

The K-Ni-Co-F or AC electrodes were fabricated by simply pressing the mixture of

70 wt% sample, 20 wt% acetylene black (AB) and 10 wt% polyvinylidene fluoride (PVDF, which was dissolved in into the N-methyl-2-pyrrolidone (NMP)) into the nickel foam (NF), which were then dried at 100 °C for 12 h in an oven. The mass loading of electroactive materials was about 4 mg cm^{-2}. The AC//K-Ni-Co-F asymmetric supercapacitors were assembled with commercial AC and as-prepared K-Ni-Co-F as negative and positive active materials, and the mass ratio of AC/K-Ni-Co-F was designed on the basis of the charge-balance ($Q+ = Q-$), as shown in equation (1) and Table S2.

The electrochemical performances were examined by cyclic voltammetry (CV), galvanostatic charge-discharge (GCD) and cycle life tests at room temperature. Tests for the K-Ni-Co-F and AC electrodes were conducted in a three-electrode cell equipped with a K-Ni-Co-F or AC working electrode (WE), a platinum plate counter electrode (CE) and a Hg/HgO (1 M KOH) reference electrode (RE). Tests for the AC//K-Ni-Co-F asymmetric capacitors were measured by two-electrode coin cells (type 2032). The electrolytes in the experiment were the 3 M KOH+0.5 M LiOH solutions. The specific capacity (C_m, mAh g^{-1}), energy density (E_m, Wh Kg^{-1}) and power density (P_m, KW Kg^{-1}) were calculated according to the equations (2), (3) and (4).

$$\boldsymbol{m\,(+)\,/\,m\,(-) = Q_m\,(-)\,/\,Q_m\,(+)} \tag{1}$$

$$\boldsymbol{C_m = Q_m\,/\,3.6 = I\,t_d\,/\,3.6\,m} \tag{2}$$

$$\boldsymbol{E_m = (C_m \Delta V)\,/\,2} \tag{3}$$

$$\boldsymbol{P_m = 3.6\,E_m\,/\,t_d} \tag{4}$$

Where m, Q_m, ΔV, I and t_d refer to the mass of active materials (g) (for supercapacitors, it means the total masses of active materials of negative and positive electrodes), specific charge quantity (C g^{-1}), potential window (V), current (A) and discharging time (s) respectively.

Fig. S1　EDS data of K-Ni-Co-F sample (Ni/Co=4:1)：the SEM image of testing area (a), EDS spectra (b) and quantitative analysis (c).

a

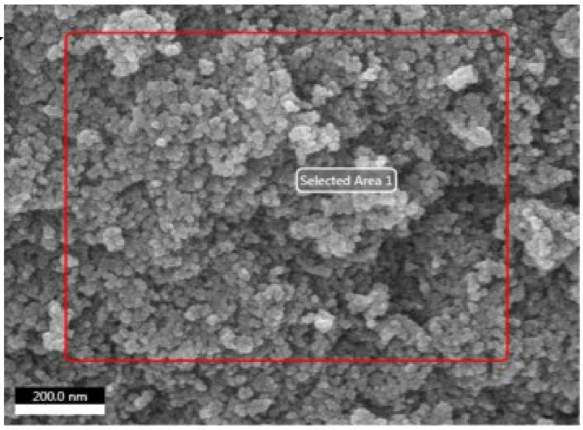

b

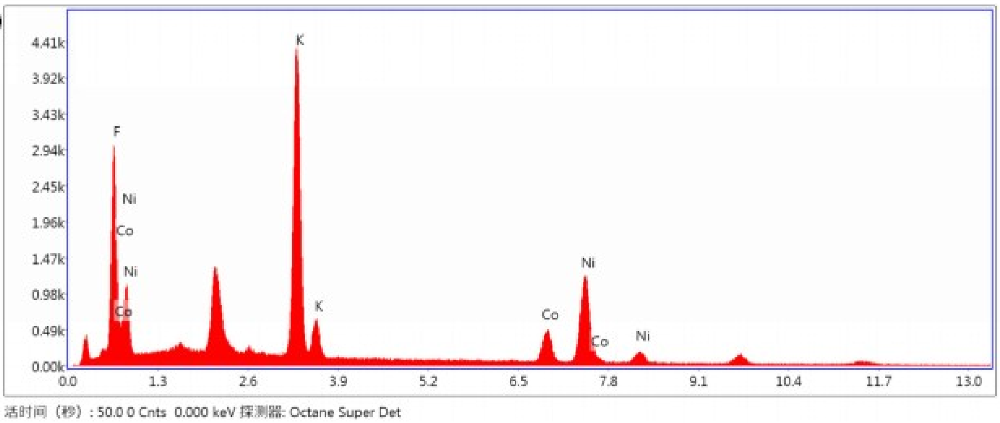

c

Element	wt%	At%	Net Intensity	Error %	Kratio	Z	R	A	F
F K	27.90	50.03	511.90	8.37	0.10	1.1	0.92	0.33	1
K K	28.00	24.40	1,021.85	2.35	0.26	1.01	1	0.92	1.02
CoK	10.53	6.09	134.56	4.64	0.10	0.9	1.04	0.99	1.03
NiK	33.57	19.48	377.69	2.75	0.31	0.93	1.04	0.99	1

Fig. S2 F1s, K2p, Ni2p, Co2p spectra of K-Ni-Co-F samples (Ni/Co=1:0, 4:1, 0:1).

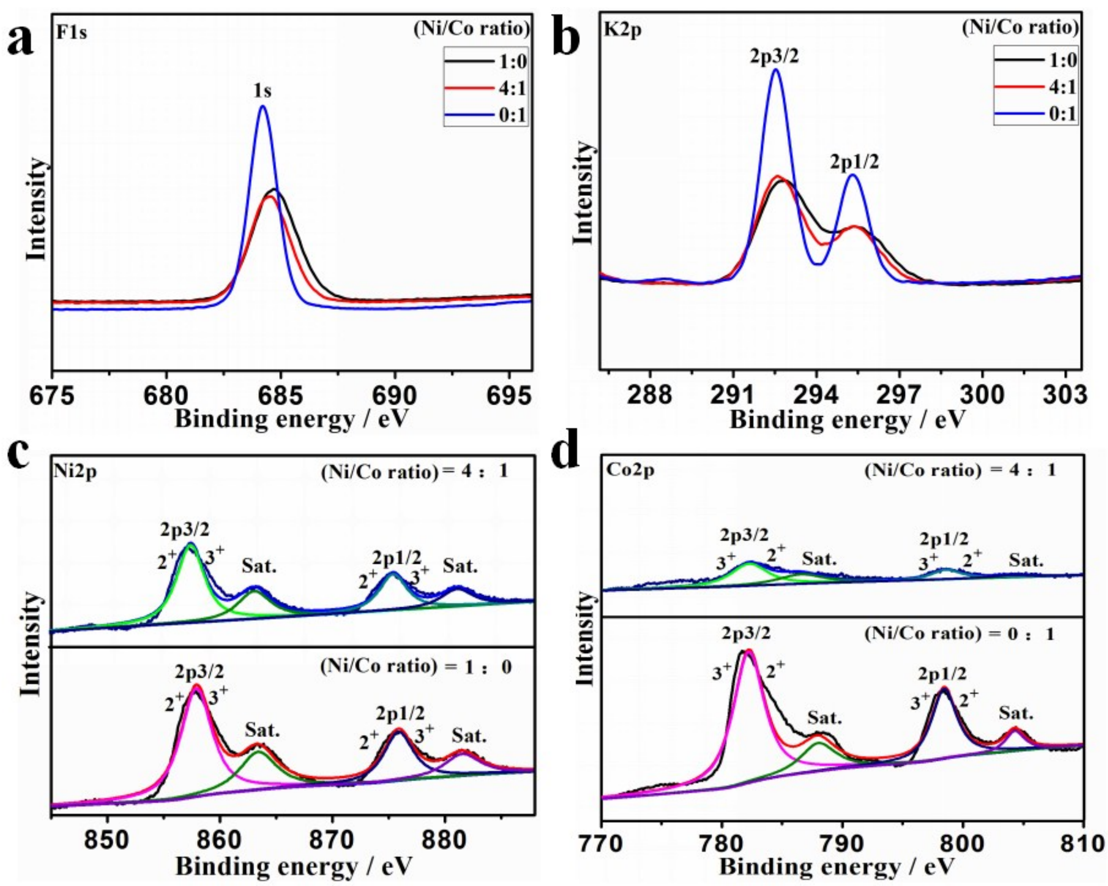

Fig. S3 **SEM / TEM images of K-Ni-Co-F samples with Ni/Co ratios of 1:0 (a, d / g, j), 4:1 (b, e / h, k) and 0:1 (c, f / i, l).**

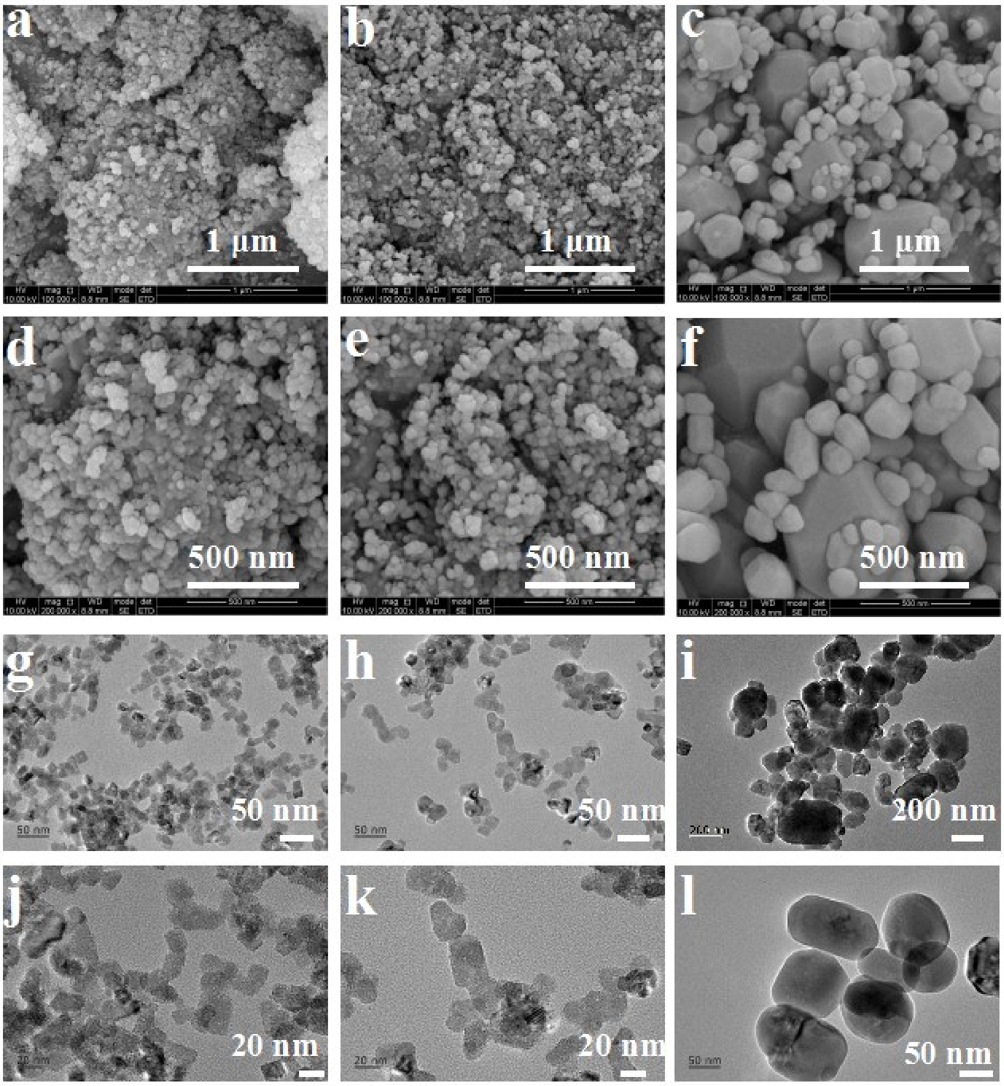

Fig. S4 GCD curves at 1~16 A g^{-1} of K-Ni-Co-F (Ni/Co=1:0, 8:1, 4:1, 2:1, 1:1, 1:2, 0:1) (a-g) and AC (h) electrodes.

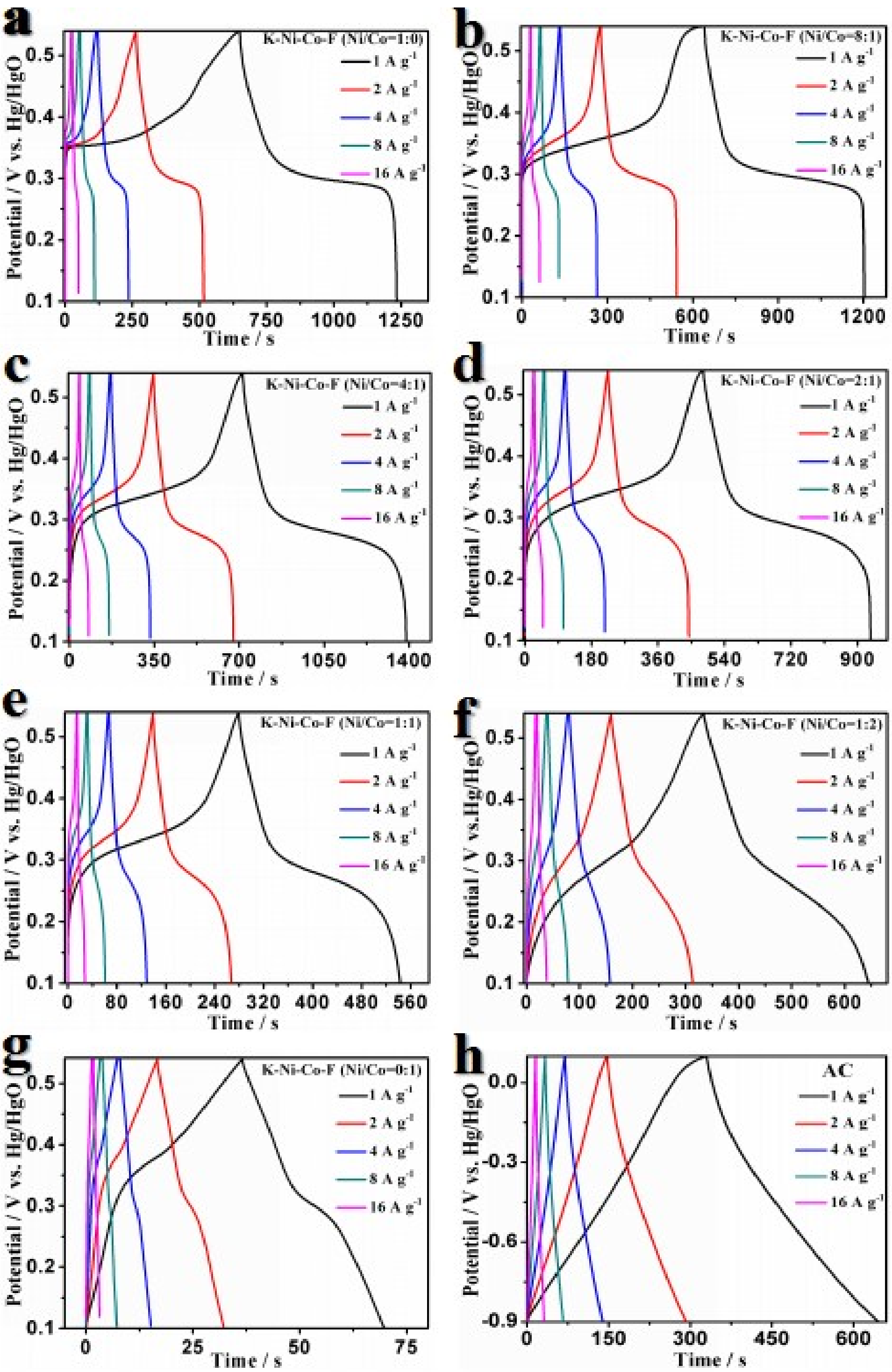

Fig. S5 CV windows at 30 mV s^{-1} (a-c) and GCD curves 1~64 A g^{-1} (d-f) of AC//K-Ni-Co-F (Ni/Co=1:0, 0:1, 4:1) asymmetric capacitors.

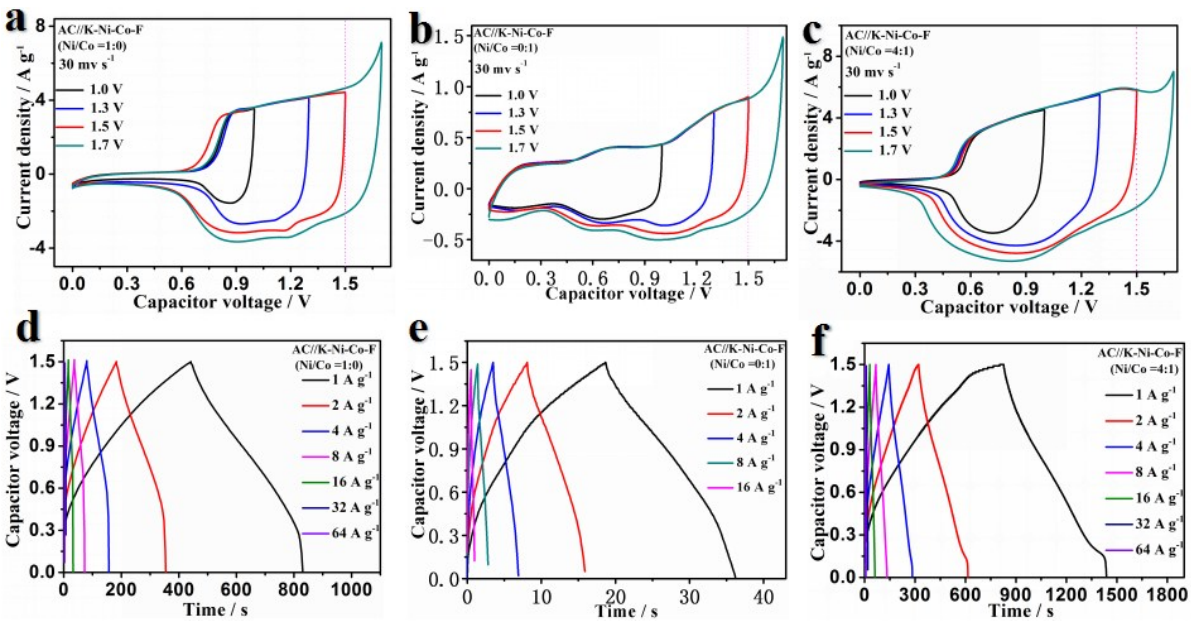

Table S1 Performance comparison of the perovskite K-Ni-Co-F (Ni/Co=4:1) materials with some reported perovskite oxides and other types of state-of-art electrode materials.

Electrode materials	Specific capacity or specific capacitance (mAh g^{-1}/C g^{-1} or F g^{-1})	Current density or Scan rate (A g^{-1}; mV s^{-1})	Electrolytes	Refs.
Perovskite oxides				
$SrRuO_3$; $La_{0.2}Sr_{0.8}Mn_{0.2}Ru_{0.8}O_3$	270 F g^{-1}; 160 F g^{-1}	20 mV s^{-1}	6 M KOH	[7]
$BiFeO_3$	81~45 F g^{-1}	20~200 mV s^{-1}	1 M NaOH	[8]
$TiO_2/BiFeO_3$	440~352 F g^{-1}	1.1~2.5 A g^{-1}	0.5 M Na_2SO_4	[9]
$LaNiO_3$; $MnO_x/LaNiO_3$	6.2~5.8; 160~78 F g^{-1}	10~50; 0.01~1 V s^{-1}	1 M Na_2SO_4	[10]
$LaNiO_3$	422~278 F g^{-1}	1~20 A g^{-1}	6 M KOH	[11]
$LaMO_3$ (M=Ni, Mn, Fe, Cr)	106.58, 56.78, 16.43, 24.40 F g^{-1}	1 A g^{-1}	3 M LiOH	[12]
$LaNiO_3/NiO$	213.2~177.8 F g^{-1}	1~5 A g^{-1}	7 M KOH	[14]
$La_{0.85}Sr_{0.15}MnO_3$; $LaMnO_3$	198~85; 187~60 F g^{-1}	0.5~3 A g^{-1}	1 M KOH	[15]
$(La_{0.75}Sr_{0.25})_{0.95}MnO_{3-\delta}$	56 F g^{-1}	2 mV s^{-1}	1 M Na_2SO_4	[16]
$La_xSr_{1-x}NiO_{3-\delta}$	719~505 F g^{-1}	2~20 A g^{-1}	1 M Na_2SO_4	[17]
$La_xSr_{1-x}Co_{0.1}Mn_{0.9}O_{3-\delta}$	485 F g^{-1}	1 A g^{-1}	1 M KOH	[18]
Other types of materials				
$Ni_{0.67}Co_{0.33}Se$	535~425 C g^{-1}	1~15 A g^{-1}	6 M KOH	[26]
Ni-Co-P	1448~1173 F g^{-1}	1~16 A g^{-1}	3 M KOH + 0.5 M LiOH	[27]
Ni-Co-F	564~418 F g^{-1}	1~16 A g^{-1}	3 M KOH + 0.5 M LiOH	[28]
$NiCo_2O_4$	351~288 F g^{-1}	1~8 A g^{-1}	6 M KOH	[29]
Ni-P@$NiCo_2O_4$	1240~668 F g^{-1}	1~16 A g^{-1}	3 M KOH + 0.5 M LiOH	[30]
$Ni_xCo_{2-x}P$	571~416 C g^{-1}	1~20 A g^{-1}	6 M KOH	[31]
$CoMoO_4$-$NiMoO_4$•xH_2O	1039~826 F g^{-1}	0.625~12.5 A g^{-1}	2 M KOH	[32]
$NiCo_2S_4$@$Ni_3V_2O_8$	512~396 C g^{-1}	1~10 A g^{-1}	6 M KOH	[33]
$NiCo_2S_4/Co_9S_8$	749~620 F g^{-1}	4~15 A g^{-1}	6 M KOH	[34]
$NiCo_2O_4$@$NiWO_4$	1384~1183.3 F g^{-1}	1~10 A g^{-1}	6 M KOH	[35]
Co–Ni–W–B–O/20rGO	1189.1~668.1 F g^{-1}	1~15 A g^{-1}	6 M KOH	[36]
OMC/MoO_2	37~17 mAh g^{-1}	0.2~2 A cm^{-2}	1 M H_2SO_4	[37]
OMC/WO_{3-x}	175~135 F g^{-1}	0.2~2 A cm^{-2}	1 M H_2SO_4	[38]
K-Ni-Co-F (Ni/Co=4:1)	**187~172 mAh g^{-1}; 673~619 C g^{-1}; 1530~1407 F g^{-1}**	**1~16 A g^{-1}**	**3 M KOH + 0.5 M LiOH**	**This work**

Table S2 The design of m_{-}/m_{+} ratios of AC//K-Ni-Co-F (Ni/Co=1:0, 0:1, 4:1) asymmetric capacitors.

Supercapacitors	Q_m (C g^{-1}) / (1 A g^{-1})				m_{-} / m_{+}
	AC	K-Ni-Co-F (Ni/Co=1:0)	K-Ni-Co-F (Ni/Co=0:1)	K-Ni-Co-F (Ni/Co=4:1)	
AC//K-Ni-Co-F (Ni/Co=1:0)	314	583	/	/	1.9/1
AC//K-Ni-Co-F (Ni/Co=0:1)		/	33	/	1/9.5
AC//K-Ni-Co-F (Ni/Co=4:1)		/	/	673	2.1/1

Table S3 Performance comparison of the AC//K-Ni-Co-F (Ni/Co=4:1) asymmetric capacitor of this work with some reported state-of-art asymmetric supercapacitors

Asymmetric Supercapacitors	**Working voltage (V)**	**Energy density (Wh Kg^{-1})**	**Power density (KW Kg^{-1})**	**Cycling stability Retention / cycles/ current density or scan rates**	**Refs.**
AC//Ni-Co-F	1.5	18.4	6.64	77% / 10,000 cycles / 4 A g^{-1}	[28]
AC//$NiCo_2O_4$	1.4	6.8	2.8	64% / 5,000 cycles / 1.5 A g^{-1}	[29]
AC//Ni-P@$NiCo_2O_4$	1.5	13.3	5.7	78% / 10,000 cycles / 4 A g^{-1}	[30]
AC//Ni-Co-P	1.5	18	5.586	91.8% / 3,000 cycles / 2 A g^{-1}	[31]
AC//$CoMoO_4$-$NiMoO_4$•$x$$H_2O$	1.4	15.5	1.64	65% / 1,000 cycles / 2.5 A g^{-1}	[32]
AC//$NiCo_2S_4$@$Ni_3V_2O_8$	1.6	14.7	8.0	94% / 5,000 cycles / 3 A g^{-1}	[33]
AC//$NiCo_2S_4$/Co_9S_8	1.5	33.5	0.15	70% / 10,000 cycles / 1 A g^{-1}	[34]
rGO//Co–Ni–W–B–O/20rGO	1.5	25.3	4.389	79.4% / 10,000 cycles / 5 A g^{-1}	[36]
AC//Ni-P	1.6	11.8	8	85% / 1,000 cycles / 5 A g^{-1}	[39]
AC//$NiWO_4$	1.6	15.1	4.8	91% / 5,000 cycles / 1 A g^{-1}	[40]
Porous C//$NiCo_2S_4$	1.5	10.6	2.47	77% / 5,000 cycles / 5 mA cm^{-2}	[41]
AC//ZTO@Ni-Co-LDHs	1.2	9.7	5.82	92.7% / 5,000 cycles/ 50 mV s^{-1}	[42]
AC//K-Ni-Co-F (Ni/Co=4:1)	**1.5**	**40; 33; 18.8; 13.8;**	**0.484; 3.88; 7.5; 18.8;**	**98% / 10,000 cycles / 4 A g^{-1}**	**This work**

The references in the Tables S1, S3:

[7] M. W. Mehrens, J. Schenk, P. M. Wilde, E. Abdelmula, P. Axmann and J. Garche, New materials for supercapacitors, *J. Power Sources*, 2002, **105**, 182–188.

[8] C. D. Lokhande, T. P. Gujar, V. R. Shinde, Rajaram S. Mane and S. H. Han, Electrochemical supercapacitor application of pervoskite thin films, *Electrochim. Commun.*, 2007, **9**, 1808–1809.

[9] A. Sarkar, A. K. Singh, D. Sarkar, G. G. Khan, K. Mandal, Three-Dimensional Nanoarchitecture of $BiFeO_3$ Anchored TiO_2 Nanotube Arrays for Electrochemical Energy Storage and Solar Energy Conversion, *ACS Sustainable Chem. Eng.*, 2015, **3**, 2254–2263.

[10] D K Hwang, S Kim, J H Lee, I.S. Hwang, I.D. Kim, Phase evolution of perovskite $LaNiO_3$ nanofibers for supercapacitor application and p-type gas sensing properties of LaOCl–NiO composite nanofibers. *J. Mater. Chem.*, 2011, 21, 1959–1965.

[11] T. Y. Shao, H. H. You, Z. J. Zhai, T. H. Liu, M. Li and L. Zhang, Hollow spherical $LaNiO_3$ supercapacitor electrode synthesized by a facile template-free method, *Mater. Lett.*, 2017, **201**, 122–124.

[12] N. Arjun, G. T. Pan and T. C.K. Yang, The exploration of Lanthanum based perovskites and Their complementary electrolytes for the supercapacitor applications, *Results Phys.*, 2017, **7**, 920–926.

[13] L. Hu, Y. F. Deng, K. Liang, X. J. Liu and W. C. Hu, $LaNiO_3$/NiO hollow nanofibers with mesoporous wall: a significant improvement in NiO electrodes for supercapacitors, *J. Solid State Electrochem.*, 2015, **19**, 629–637.

[14] K. Liang, N. Wang, M. Zhou, Z. Y. Cao, T. L. Gu, Q. Zhang, X. Z. Tang, W. C. Hu and B. Q. Wei, Mesoporous $LaNiO_3$/NiO nanostructured thin films for high-performance supercapacitors, *J. Mater. Chem. A*, 2013, **1**, 9730–9736.

[15] X. W. Wang, Q. Q. Zhu, X. E. Wang, H. C. Zhang, J. J. Zhang and L. F. Wang, Structural and electrochemical properties of $La_{0.85}Sr_{0.15}MnO_3$ powder as an electrode material for supercapacitor, *J. Alloys Compds.*, 2016, **675**, 195–200.

[16] J. B. Lü,Y. H. Zhang, Z. Lü, X. Q. Huang, Z. H. Wang, X. B. Zhu and B. Wei, A preliminary

study of the pseudo-capacitance features of strontium doped lanthanum manganite, *RSC Adv.*, 2015, **5**, 5858–5862.

[17] Y. Cao, B. P. Lin, Y. Sun, H. Yang and X. Q. Zhang, Sr-doped Lanthanum Nickelate Nanofibers for High Energy Density Supercapacitors, *Electrochim. Acta*, 2015, **174**, 41–50.

[18] Y. Cao, B. P. Lin, Y. Sun, H. Yang and X. Q. Zhang, Structure, morphology and electrochemical properties of $La_xSr_{1-x}Co_{0.1}Mn_{0.9}O_{3-\delta}$ perovskite nanofibers prepared by electrospinning method, *J. Alloys Compds.*, 2015, **624**, 31–39.

[26] H. C. Chen, S. Chen, M. Q. Fan, C. Li, D. Chen, G. L. Tian and K. Y. Shu, Bimetallic nickel cobalt selenides: a new kind of electroactive materials for high-power energy storage, *J. Mater. Chem. A*, 2015, **3**, 23653–23659.

[27] R. Ding, X. D. Li, W. Shi, Q. L. Xu and E. H. Liu, One-pot solvothermal synthesis of ternary Ni-Co-P micro/nano-structured materials for high performance aqueous asymmetric supercapacitors, *Chem. Eng. J.*, 2017, **320**, 376–388.

[28] X. D. Li, R. Ding, W. Shi, Q. L.Xu and E. H. Liu, Ternary Ni-Co-F Nanocrystal-Based Supercapacitors. *Chem. Eur. J.*, 2017, **23**, 6896–6904.

[29] R. Ding, L. Qi, M. J. Jia and H. Y. Wang, Facile and large-scale chemical synthesis of highly porous secondary submicron-micron-sized $NiCo_2O_4$ materials for high-performanceaqueous hybrid AC-$NiCo_2O_4$ electrochemical capacitors, *Electrochim. Acta*, 2013, **107**, 494–502.

[30] X. D. Li, R. Ding, L. H. Yi, W. Shi, Q. L. Xu and E. H. Liu, Mesoporous Ni-P@$NiCo_2O_4$ composite materials for high performance aqueous asymmetric supercapacitors, *Electrochim. Acta*, 2016, **222**, 1169–1175.

[31] Y. M. Hu, M. C. Liu, Y. X. Hu, Q. Q. Yang, L. B. Kong and L. Kang, One-pot hydrothermal synthesis of porous nickel cobalt phosphides with high conductivity for advanced energy conversion and storage, *Electrochim. Acta*, 2016, **215**, 114–125.

[32] M. C. Liu, L. B. Kong, C. Lu, X. J. Ma, X. M. Li, Y. C. Luo and L. Kang, Design and synthesis of $CoMoO_4$–$NiMoO_4$•$x$$H_2O$ bundles with improved electrochemical properties for supercapacitors. *J. Mater. Chem. A*, 2013, **1**, 1380–1387.

[33] L. Y. Niu, Y. D. Wang, F. P. Ruan, C. Shen, S. Shan, M. Xu, Z. K. Sun, C. Li, X. J. Liu and Y. Y Gong, *In situ* growth of $NiCo_2S_4$@$Ni_3V_2O_8$ on Ni foam as a binder-free electrode for asymmetric supercapacitors, *J. Mater. Chem. A*, 2016, **4**, 5669–5677.

[34] L. R. Hou, Y. Y. Shi, S. Q. Zhu, M. Rehan, G. Pang, X. G. Zhang and C. Z. Yuan, Hollow mesoporous hetero-$NiCo_2S_4/Co_9S_8$ submicro-spindles: unusual formation and excellent pseudocapacitance towards hybrid supercapacitors, *J. Mater. Chem. A*, 2017, **5**, 133–144.

[35] S. M. Chen, G. Yang, Y. Jia and H. J. Zheng, Three-dimensional $NiCo_2O_4$@$NiWO_4$ core–shell nanowire arrays for high performance supercapacitors. *J. Mater. Chem. A*, 2017, **5**, 1028–1034.

[36] C. L. Xiang, Q. Y. Wang, Y. J. Zou, P. R. Huang, H. L. Chu, S. J. Qiu, F. Xu and L. X. Sun, Simple synthesis of graphene-doped flower-like cobalt–nickel–tungsten–boron oxides with selfoxidation for high-performance supercapacitors, *J. Mater. Chem. A*, 2017, **5**, 9907–9916.

[37] Y. Zhou, C. W. Lee and S. Yoon, Development of an Ordered Mesoporous Carbon/MoO_2 Nanocomposite for High Performance Supercapacitor Electrode, *Electrochem. Solid-State Lett.*, 2011, **14**, A157–A160.

[38] Y. Zhou, S. Ko, C. W. Lee, S.G. Pyo, S.-K. Kim and S. Yoon, Enhanced charge storage by optimization of pore structure in nanocomposite between ordered mesoporous carbon and nanosized WO_{3-x}, *J. Power Sources*, 2013, **244**, 777–782.

[39] D. Wang, L. B. Kong, M. C. Liu, W. B. Zhang, Y. C. Luo and L. Kang, Amorphous Ni-P materials for high performance pseudocapacitors, *J. Power Sources,* 2015, **274**, 1107–1113.

[40] L. Y. Niu, Z. P. Li, Y. Xu, J. F. Sun, W. Hong, X. H. Liu, J. Q. Wang and S. R. Yang, Simple synthesis of amorphous $NiWO_4$ nanostructure and its application as a novel cathode material for asymmetric supercapacitors, *ACS Appl. Mater. Interfaces.,* 2013, **5**, 8044–8052.

[41] W. Kong, C. C. Lu, W. Zhang, J. Pu and Z. H. Wang, Homogeneous core–shell $NiCo_2S_4$
nanostructures supported on nickel foam for supercapacitors. *J. Mater. Chem. A*, 2015, **3**, 12452–12460.

[42] X. Wang, A. Sumboja, M. F. Lin, J. Yan and P. S. Lee, Enhancing electrochemical reaction sites in nickel–cobalt layered double hydroxides on zinc tin oxide nanowires: a hybrid material for an asymmetric supercapacitor device, *Nanoscale*, 2012, **4**, 7266–7272.